Open Access

OBM Genetics

LIDSEN Publishing Inc.

Original Research

Chest CT Scan Features of COVID-19 in a Hospitalized High-Altitude Population

Walter Calderón Gerstein [1, ‡, *], Gabriela Torres Samaniego [2], Kevin Pazos Sovero [3]

1. School of Medicine, Universidad Continental, Huancayo, Peru; E-Mail: wcalderon@continental.edu.pe
2. Puesto de Salud San Pedro de Cajas, EsSalud, Tarma, Peru; E-Mail: gabrielaktorress@gmail.com
3. Centro de Salud Juan Parra del Riego, Huancayo, Peru; E-Mail: pazossoverokevinantony@gmail.com

‡ Current Affiliation: Internal Medicine Service, Hospital Nacional Ramiro Prialé Prialé, EsSalud, Huancayo, Peru

* **Correspondence:** Walter Calderón Gerstein; E-Mail: wcalderon@continental.edu.pe

Academic Editor: Thomas Liehr

Special Issue: Oxygen Transport Physiology and COVID at High Altitude

OBM Genetics
2024, volume 8, issue 2
doi:10.21926/obm.genet.2402226

Received: November 30, 2022
Accepted: March 14, 2024
Published: April 12, 2024

Abstract

There is a lack of knowledge regarding the type of lung compromise in high-altitude residents with COVID-19. This study aims to evaluate the lung compromise in chest CT scans of high-altitude dwellers hospitalized with COVID-19. Retrospective study that took place in "Daniel Alcides Carrión" Regional Hospital, located 3,250 meters above sea level in the city of Huancayo, Perú. 464 medical charts and chest CT images of hospitalized patients with confirmed COVID-19 from January to March 2021 were reviewed. The mean age was 56 years, 63.1% of the patients were male, and 85.8% of individuals had a CORADS 5. Ground glass infiltrates were found in 93.8% of the patients; alveolar consolidations were present in 86% and were usually bilateral. Thickened septa were described in 46%, lattice pattern in 38.8%, reticular components in 39%, and the crazy paving pattern in 36.9%. Most patients (84.5%)

had central and peripheral lesions; only 4% had limited peripheral compromise, and 10% solely central distribution. The left posterior basal segment was the most affected pulmonary segment in 27% of the cases, and the right basal posterior in 26%. Less affected segments were the right and left apical (14% and 13%, respectively). Lung compromise in patients with COVID-19 in this high-altitude population was severe, with mostly bilateral compromise, increased diameter of the pulmonary artery, periaortic and subaortic lymph nodes enlargement, and extensive ground glass and alveolar lesions.

Keywords
COVID-19; high altitude; chest CT scan; ground glass infiltrates

1. Introduction

In December 2019, new cases of pneumonia of unknown origin were reported in Wuhan (China). On January 7, 2020, the causative agent of this new disease, called new coronavirus 2019 (2019-nCoV), was identified. On February 11 of the same year, the World Health Organization (WHO) named it coronavirus disease 2019 (COVID-19) caused by a new type of coronavirus, SARS-CoV-2 [1].

COVID-19 infection clinical presentation can be mild, moderate, or severe; in some cases, it can cause severe pneumonia, acute respiratory distress syndrome, sepsis, and in severe forms, septic shock can be evidenced [2, 3].

The respiratory system is the first to be affected by the SARS-CoV-2 virus, and, in suspected cases, false negative results have been reported with serological antibody tests and even with RT-PCR in the initial stages of the disease [4-6]. Therefore, lung CT scans play a crucial role in these cases of COVID-19 since there is much evidence of the usefulness of tomography as a diagnostic test in the absence of RT-PCR [7, 8]. In addition, the sensitivity of chest tomography is much higher compared to RT-PCR in the diagnosis of COVID-19 [9].

Tomographic findings have become fundamental in diagnosing COVID-19, particularly in its initial phases or before the appearance of symptoms. Determining the different types of lung infiltrates and patterns has proved very useful for evaluating the course of the disease [10, 11]. The most common tomographic lesions are bilateral ground glass opacities, reticulonodular patterns, and crazy-paving infiltrates [5, 12, 13]. However, chest tomography findings in COVID-19 in high altitude populations have not been reported previously. Moreover, the effect of high altitude on COVID-19 survival continues under discussion [14, 15]. This study aims to determine the tomographic findings in patients hospitalized with COVID-19 in a high-altitude hospital.

2. Materials and Methods

This study is descriptive, observational, and retrospective. A total of 464 clinical charts, along with their corresponding chest computed tomography findings, were evaluated. All patients had COVID-19 confirmation with RT-PCR or antigen test, or both. The individuals were admitted to the Internal Medicine wards or the Intensive Care Unit of the "Daniel Alcides Carrión" Regional Clinical-Surgical Teaching Hospital from January to March 2021. Carrión Hospital is located in Huancayo, a

Peruvian city at 3,250 meters above sea level (masl). All patients had COVID-19 confirmation with RT-PCR or antigen test, or both.

2.1 Chest CT Scan

Chest CT scans, spiral, ungated, and non-enhanced, were acquired with low-dose, on one CT scanner, a 128-slice system (Hitachi Scenaria View 2020). Scan parameters for Hitachi Scenaria included tube voltage of 140 kV, 0.35-second rotation speed, and slice thickness of 1 mm. CT scans were acquired from two slices above the lung apex to three slices down costophrenic angles during a single inspiratory breath-hold.

The Fleischner Society glossary for thoracic imaging was utilized to identify chest CT lesion patterns. COVID-19 pneumonia was diagnosed based on ground-glass opacities, consolidations, and crazy-paving patterns, which were integrated into the CORADS score.

The research instrument was the data collection form, which was filled out by the researchers using the clinical chart data and the chest CT scan results of patients with COVID-19. All chest CT scans were evaluated and informed by trained radiologists.

This study complies with the principles of the Declaration of Helsinki for medical research involving human subjects. The confidentiality and anonymity of the patients were secured. The Ethics Committee of Carrión's hospital approved the study on December 2, 2021, with registration number 5774479, according to the Peruvian legislation regarding observational studies in humans.

2.2 Statistical Analysis

The results are presented in tables and graphics, with calculations made for the mean, median, mode, and standard deviation.

3. Results

A total of 63.1% (n = 293) of the patients were male, while 36.9% (n = 171) were female. Of the patients evaluated, 40.7% were older adults (n = 189). Diagnosis was made in 73.7% of the patients through antigen testing and 26.3% through molecular testing (RT-PCR). The average age was 56.14 years, with a minimum of 21 and a maximum of 94 years.

3.1 Comorbidities

The most frequent comorbidity was obesity, found in 40.3% (n = 187), followed by diabetes mellitus 2 in 20.9% (n = 97), and hypertension, diagnosed in 17% (n = 79). Cardiovascular and chronic lung disease rates were low, with only four patients with each of these characteristics (0.9%). There were only 6 patients with immunosuppressive treatment (1.3%), 8 asthmatics (1.7%), and one patient with HIV infection (Table 1).

Table 1 Comorbidities in COVID-19 patients.

Pathological history	No.	Percentage
Obesity	187	40.3
Diabetes mellitus type 2	97	20.9

Hypertension	79	17.0
Chronic renal insufficiency	12	2.6
Asthma	8	1.7
Immunosuppressant treatment	6	1.3
cardiovascular disease	4	0.9
Chronic lung disease	4	0.9
HIV infection	1	0.2

Place of origin: 80% of the patients (n = 371) came from the city of Huancayo, and 10% (n = 46) from the neighboring areas of the Mantaro Valley (Concepción 3,283 masl, Chupaca 3,263 masl, and Jauja 3,335 masl).

The average Body Mass Index (BMI) was 28.94 kg/m^2; the average oxygen saturation was 78.54%, with a minimum of 35 and a maximum of 94%. The average respiratory rate was 23.55 resp/min, the average heart rate was 94.14 beats/min, and the average temperature was 37.11°C.

3.2 Clinical Presentation

The main symptom was dyspnea, found in 89.2% (n = 414), followed by cough (73.1%) and fever (63.1%). The average hospital stay was 9.30 days, with a minimum of 2 and a maximum of 48 days.

3.3 Laboratory Tests

On average, the CRP (C reactive protein) values were 136.3 mg/dL, with a maximum value of 546.8 mg/dL. The D-dimer mean value was 2448.10 ng/mL, reaching 100,000 in one case and 231 ng/mL in another patient. Lactate dehydrogenase (LDH) averaged 538.97 U, while creatinine averaged 1.04 mg/dL and albumin 3.44 mg/dL. Platelets' mean value was 26,880/mm^3, white blood cell count was 11,155/mm^3, lymphocytes 967/mm^3, and neutrophils 9,609/mm^3.

3.4 Complications

The main complications observed are shown in Figure 1.

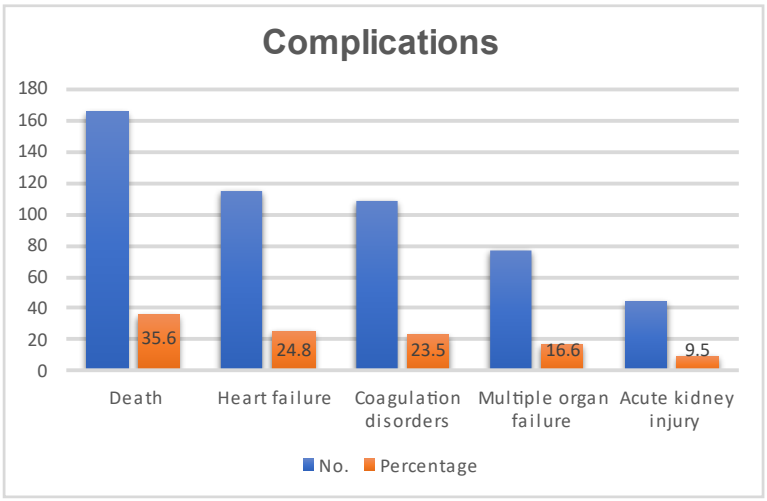

Figure 1 Complications in hospitalized patients with COVID-19.

3.5 Lung Injury Patterns

The most frequently found lesion was the ground glass pattern, present in 93.8% (n = 435) of the patients, followed by alveolar consolidations in 86.2% (n = 400).

Figure 2 shows a bilateral ground glass pattern in a male patient as the most common chest CT abnormality in the evaluated population. Figure 3 shows bilateral consolidations in a patient; this was the second most common abnormal pattern found.

Figure 2 Bilateral ground-glass pattern in a 53-year-old man.

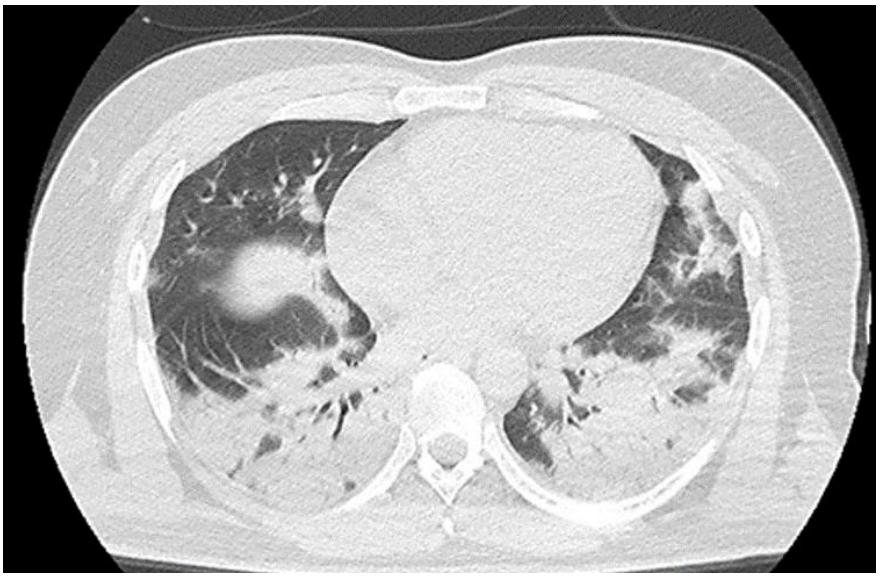

Figure 3 Bilateral consolidations in a male patient.

The presence of thickened septa was observed in 46.1%, the reticular pattern in 38.8%, and the crazy cobblestone pattern in 36.9%. 35.3% of patients presented vascular dilatations. Paratracheal nodes were observed in 27.4% of the cases, subaortic nodes in 17.9%, and calcified nodules in 12.5%. Atelectasis was observed in 12.3% (N = 57), and 13 patients (2.8%) presented pleural effusion (Table 2).

Table 2 Patterns of lung injury found in the study population.

Patterns of lung injury	No.	Percentage
Ground glass pattern	435	93.8
Alveolar consolidations	400	86.2
Thickened septa	214	46.1
Lattice pattern	180	38.8
Crazy paving pattern	171	36.9
Presence of vascular dilation	164	35.3
Paratracheal nodes	127	27.4
Subaortic nodes	83	17.9
Calcified nodules	58	12.5
Atelectasis	57	12.3
Pleural effusion	13	2.8
Microcysts	9	1.9

3.6 Location of Pulmonary Lesions

Bilateral consolidation was the predominant one in 71.6% (n = 332). The most frequent ground glass pattern was subpleural (53.2%), finding bilateral lesions in 54.5%. 23.3% of patients showed the presence of multiple lesions in different lobes. About the most affected segments, the most frequent location was the left posterior basal segment (27.6%), followed by the right basal posterior segment (26.5%), as well as the right apical segment (13.8%) and the left apical segment (12.7%) (Table 3).

Table 3 Predominant Location of Lung Lesions.

Lung injury pattern	No.	Percentage
Bilateral consolidation	332/463	71.6
Subpleural ground glass	247	53.2
Two-sided ground glass	253	54.5
Left posterior basal segment	128	27.6
Right posterior basal segment	123	26.5
Multilobar Compromise	108/463	23.3
Right apical segment	64	13.8
Left apical segment	59	12.7

Mode of distribution of the lesions: 84.5% had both central and peripheral distributions. In only 48 patients (10.3%), the distribution was exclusively central; in only 19 patients (4.1%), the distribution was exclusively peripheral.

CORADS Classification: 85.8% of patients (n = 398) had a CORADS score of 5, followed by 6.9% of cases with CORADS 4 and 2.8% of cases with CORADS 3. Only 1.5% of cases had CORADS 6 or CORADS 1, and only two patients showed CORADS 2 type lesions.

Mean Pulmonary Artery Diameter: The average PA diameter evaluated according to chest tomography was 27.6 mm, with a minimum value of 18 mm and a maximum of 38 mm.

Phases of progression of lung lesions: In most cases, the peak phase (44.6%) was predominant during the tomography evaluation (Table 4).

Table 4 Phases of lung disease progression.

Phase	No.	Percentage
Peak phase	207	44.6
Progressive phase	130	28.0
Peak and absorptive phase	38	8.2
Peak and progressive phase	26	5.6
Absorptive phase	24	5.1
Total	425	100.0

3.7 Distribution of Lung Lesions

The lung lobes with a higher percentage of involvement by COVID-19 lesions were the right lower lobe (45.5%) and the left lower lobe (44.4%). The percentage of compromise of the right upper lobe and the middle lobe was around 34%, and of the left upper lobe, 33.4% (Table 5).

Table 5 Ratio of Lung Compromise in different lobes.

	Minimum Lung Compromise (%)	Maximum Lung Compromise (%)	Average Lung Compromise (%)
Right upper lobe	0	100	34.11
Medium lobe	0	100	34.14
Right lower lobe	10	100	45.51
Left upper lobe	0	90	33.40
Left lower lobe	10	95	44.40
5-Lobes Lung Compromise	5	99	52.03

85.6% (n = 397) of the lesions had both central and peripheral distributions. In only 48 of the patients (10.3%), the distribution was exclusively central, and in only 19 patients (4.1%), the distribution was exclusively peripheral (Figure 4).

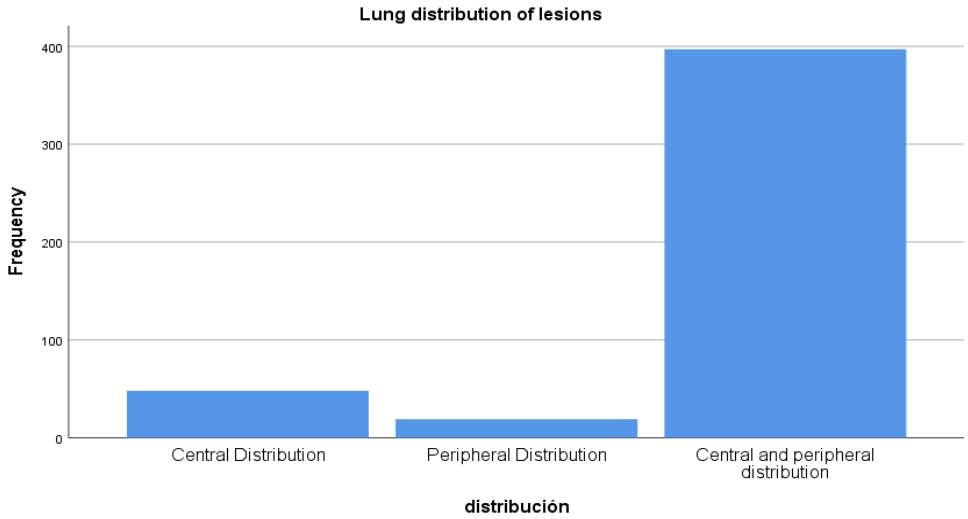

Figure 4 Mode of distribution of lung lesions.

4. Discussion

464 medical records of patients hospitalized in the medical, emergency, and intensive care unit of "Daniel Alcides Carrión" Regional Clinical-Surgical Teaching Hospital in Huancayo were evaluated. All the medical records corresponded to patients who had chest tomography evaluation upon admission to the hospital due to suspicion of having COVID-19.

The first studies evaluating the characteristics of chest CT scans in patients with COVID-19 were conducted in China. These works were generally carried out with younger populations and with less severity than that presented in this investigation. Song's study [12] was carried out with 51 patients evaluated in Shanghai hospitals, with an average age of 49 years (younger average population than that of this study) and with an almost equal proportion of men (49%) and women (51%). Xu's report [13] analyzed patients' medical records in Guangdong from January to February 2020. A total of 90 patients with an average age of 50 years were included.

The Soriano study in Spain [16] included 182 patients, whose mean age was 60 years, and males in 58.2% of the cases. This population is more similar to that of the present study since it has a slightly lower proportion of males than the one evaluated in Huancayo, a very similar average age, and a similar severity to that of the current study.

Another tomographic study on COVID-19 with a mean age and gender ratio similar to that of Huancayo patients was that of Ashtari [17], in which the author and his collaborators evaluated 363 cases in three hospitals in Iran. The average age was 61.6 years, with a male proportion of 63.8%. This study evaluated the tomographic findings in patients with mild symptoms, critical conditions, and deceased patients, as will be discussed later. The study conducted in three hospitals in China by Chung et al. [11] had a younger population with a mean age of 51 years, similar to Song's [12]. The patients were evaluated in the first days of the COVID-19 pandemic, from January 18 to 27, 2020.

The study by Escobar et al. [18] carried out as a case report of the first 14 patients who died from COVID-19 at Perú, at Rebagliati Hospital, had a population composition similar to ours, although with greater age and severity, consisting of a 78.6% by men and with an average age of 73.4 years.

Pan's study only included 63 patients, with an average age of 44.9 years [8]. The study mentioned above was carried out with CT scans evaluated during January 2020 in various locations in China.

Concerning the previous medical history, our population had a high prevalence of comorbidities. 40.3% were obese, 20.9% had type 2 diabetes mellitus, 17% hypertension, and 6% chronic kidney disease. The rate of chronic pulmonary and cardiovascular diseases was less than 3%. This rate of comorbidities is quite high when compared to the first cases of patients with COVID-19 evaluated with chest CT scans in China [12], which reported only 10% hypertensive and 6% diabetic patients. Xu series had only 6% of diabetics, with 19% hypertensive individuals and 3% patients with cardiovascular disease. In the Iranian study by Ashtari [17], comorbidities were even lower, observed in only 5.8% of the patients.

Patients from Huancayo presented with greater severity than those from China. 89.2% of the patients hospitalized for COVID-19 had dyspnea, and 63.1% came from fever. Dyspnea was observed in only 14% of cases, cough in 47% of Song's series [12], while 96% of the patients attended the clinic for fever. A similar situation was observed in another Chinese population [13], where 78% had fever, 63% cough, and no patients with dyspnea were reported. Similarly, in 95 patients from Guangdong [19], evaluated between January and February 2020, fever and fatigue were present in 72.6%, not specifically mentioning whether or not there was dyspnea. Other early CT studies on COVID-19 conducted by Chung et al. [20] showed fever in 67% of the cases without reporting the presence of dyspnea. As occurred with the greater presence of comorbidities, the older age of the patients, and the greater prevalence of males, in the Peruvian series by Escobar [18], fever and dyspnea were observed in 78.6%. In the physical examination, polypnea was found in 85.7%. This percentage is very similar to that found in the population of Huancayo, so the small series of Rebagliati cases would have a composition similar to that of the patients evaluated at Hospital Carrión. Considering that the series mentioned above of patients [18] exclusively comprises individuals who succumbed to COVID-19, it can be concluded that the disease severely impacted the population evaluated in Huancayo.

In the Carrión Hospital population, the average percentage of lung involvement was 52.03%, with maximum involvement of 99% and a minimum of 5%. The most frequently found tomographic pattern was ground glass lesions, which were present in 93.8% of the cases. 86.2% of the patients showed alveolar consolidations, 46.1% had septal thickening, 38.85% had a reticular pattern, 36.9% showed crazy cobblestone, and 35.3% had vascular dilation. Less common lesions, such as the presence of paratracheal nodes, were observed in 27.4%, subaortic in 17.9%, calcified nodules in 12.5%, atelectasis in 12.3%, pleural effusion in 2.8% and microcytes in 1.9%.

In a Chinese study [12], 77% of patients had ground glass lesions, with 75% combined with a reticular pattern and 59% with consolidation. The consolidation pattern was much less frequent than in our study, in which it was found in only 55%. In 8% of their patients, there was pleural effusion; in 6%, pericardial effusion; and a further 27%, adenopathies. Air bronchograms were found in up to 80% of the patients evaluated.

Like the study mentioned above [12], Xu [13] found ground glass lesions in 72% of cases but only 12% consolidation and 12% crazy paving. The presence of thickened septa was lower than that of Hospital Carrión, reaching only 37%, but with a pleural thickening of 56% and linear opacities of up to 61%. These linear opacities corresponded to a reticular pattern found in only 38.8% of our patients. Even more, Xu reported 23% of normal chest CT scans.

In Spain [16], ground glass-type compromise was seen in up to 60.4% of patients. The presence of lymphadenopathy was reported in 24.9%, similar to our patients, finding vascular dilation in an

even higher proportion (48.4%). Pleural effusion was observed in 7.7% of the cases and pleural thickening in 30.2% of the patients.

The Iranian study by Ashtari [21] differentiated the tomographic patterns found according to whether they were deceased or surviving patients, finding that those patients who died from COVID-19 had the combination of ground glass with consolidation in 84.6% of the cases. This lesion pattern was only observed in 38.11% of non-critical patients. Similarly, they found that up to 21.2% of deceased patients had pleural effusion. Adenopathies would also be an indicator of severity since 7.7% of the patients presented them, as opposed to 3.6% of those with mild COVID-19. This difference was statistically significant.

Sharif et al. published a meta-analysis in 2022 [22]. The researchers reviewed 86 reports of chest CT scan evaluations in COVID-19, totaling 7956 patients. The meta-analysis confirmed, as found in our population, that ground glass lesions were more frequent, reaching 73%. Unlike the Chinese studies, vascular dilatation was reported to be up to 61%, a very high rate, even for our cases, in which it was only 35%. There was a lower percentage of consolidation (34%), while pleural thickening and crazy paving were found in 24% and 27%, respectively. However, bronchiectasis had a high prevalence of 24%. As in all published case series and studies, pleural effusion and lymphadenopathy were rare. No study published to date has found such a high prevalence of adenopathies as in this population of Hospital El Carrión, in which 27.4% had the presence of enlarged paratracheal nodes and 17.9% of subaortic nodes. These adenopathies could reveal an increase in the immune response, but no studies to date associate them with greater mortality and severity.

The low prevalence of specific lesions could also be observed in the study by Zheng et al. [23], who found enlarged lymph nodes in only 3 to 13% of the patients and rarely identified vascular dilatations.

Bilateral consolidation was seen in 71.6% of our cases. Ground glass lesions were either subpleural (53.2%) or bilateral (54.2%). The involvement of the five lobes was observed only in 23.3%. The most frequent compromised lung segments were the left posterior basal (27.6%) and the right posterior basal (26.5%). The apical segments were the least compromised: the right apical with 13.8% and the left apical in 12.7% of the patients.

Song [12] reported that lesions were bilateral in 97% and all five lobes were involved in 79%; however, patients were generally not in critical condition. About the most compromised lobes, the lower lobe was compromised in 53% of the cases, followed by the upper lobes in 37% and the middle lobe in only 10% of the cases. For Salehi [5], most lesions were ground glass (88%) and were bilateral in 87.5%, compromising the five lobes in 78.8%.

The distribution of the lesions in our study was central and peripheral in 85.6% of the cases; it was exclusively central in 10.3% and only peripheral in 4.1%. This distribution pattern is important because, according to Chinese studies in patients with mild COVID-19, the peripheral distribution appears first and is seen in these non-serious cases. Xu [13] observed peripheral distribution in 51%, being bilateral in 59% of cases. In the study by Soriano in Spain, the peripheral distribution was observed at 66.7%, but it was peripheral and central only at 27.5%. In Ashtari's research [17], opacities were diffuse in 71.2% of the deceased patients, but in those who survived, and in mild cases, lesions were diffuse in only 15.5%.

Sharif's meta-analysis [22] found that the left lower lobe was involved in 67% of cases and the right in 66%, while the right middle lobe was the least commonly involved.

Most cases in our population were in the peak phase (48.7%), followed by the progressive phase in 30.59%. In some cases, a combination of phases was found, with 8.94% in the peak and absorptive phase, 6.12% in the peak and progressive phase, and 5.65% in the absorptive phase. According to Zheng et al. [23], COVID-19 patients undergo two stages: the progressive stage, which lasts from the first 3 to 14 days of the disease, and the absorptive phase, which occurs during weeks 2 to 3. The maximum pulmonary deterioration is usually observed on day 10 of hospitalization. Feng Pan [24] agrees that the maximum lung compromise occurs on the tenth day, according to a case series of 21 patients, and he suggests that the peak phase may occur between days 10 and 13 of the disease and, from day 14, the absorptive phase.

None of the patients at Carrión Hospital were in the early phase, which usually includes asymptomatic patients or those who present upper respiratory tract symptoms and have not yet developed dyspnea.

According to Kenny et al. [25], in 70% of cases, the CT scan shows lung injury before the positive molecular test. Similarly, Waller et al. [26] have reported that chest CT scans have a sensitivity of 97% for diagnosing and identifying lung lesions in COVID-19. This information is crucial since it is known that the sensitivity of the molecular test is around 70%, and the antigenic test does not reach 100% sensitivity either. Zheng et al. [23] remind us that in 60 to 93% of patients, there are abnormalities in the chest tomography before the positive molecular test. In this subject, he agrees with what was expressed by Kenny et al. [25].

The CORADS score allows for greater diagnostic certainty of the pulmonary disease and helps define who is more likely to have COVID-19 and who is not. In this population, the vast majority of patients had CORADS 5 (85.8%), indicating that the cases were quite defined and had significant lung involvement.

The most compromised lobe was the right lower lobe in 45.5%, followed by the left lower lobe in 44.4%. Unlike other studies, the involvement of the middle lobe was around 34%, as well as the upper and lower right lobes. The involvement mostly of the right lower lobe coincides with the findings reported by Salehi et al. [5], who found 76% involvement of the right lower lobe and 57% of the right middle lobe. On the other hand, Xu et al. [13] similarly found that the compromise of the right lower lobe was found in 66%, followed by the right lower lobe in 61%, results very similar to our population findings, but with the difference that the least compromised lobe was the right middle in 44% of the cases. Table 6 summarizes different studies regarding chest CT characteristics in COVID-19 patients for comparative purposes with our results.

Table 6 Table of Comparison. Chest CT Scan features of COVID-19 in different Studies.

Chest CT Scan Studies in COVID-19 Patients								
	Units							
Author		Song	Soriano	Ashtari	Escobar	Chung	Current study	Xu
Country		China	Spain	Iran	Perú	China	Perú	China
City		Shanghai	Navarra	Tehran	Lima	Zhuhai	Huancayo	Guangzhou
Reference		[12]	[16]	[17]	[18]	[20]		[13]
Number of patients		51	182	363	14	21	464	90
Mean Age	years	49	60	61.6	73.4	51	56.1	50
Male proportion	%	49	58.2	63.8	78.6	62	63.1	43.3
Presence of dyspnea	%	31			85.7	14	89.2	21
Peripheral distribution	%	86	66.7			33	4.1	51
Mixed distribution	%	2	27.5				85.6	69
Bilateral compromise	%	86	84.1	93.4	100	76	71.6	59
Ground Glass opacities	%	77	60.4	91.7	66.6	86	93.8	72
Consolidations	%	59	37.9	60.6	33.3	29	86.2	12
Crazy paving	%		54.9			19	36.9	12
Adenopathies	%	27	24.9	8		0	45.2	1
Thickened septa	%	75	37.9				46.1	37
Pleural effusion	%	8	7.7	11.3		0	2.8	4
Left lower lobe affected	%	80	27.6			67	44.4	61

Most of our cases showed exceedingly severe lung disease, as revealed by bilateral compromise, involvement of more than three lobes, the simultaneous appearance of ground glass lesions and consolidation, and the high incidence of vascular dilation and adenopathies. Most of our patients were in the peak and progressive phase; almost all had a CORADS 5 classification, and their biochemical markers revealed severe disease. The average CRP was 136 mg/dL, the mean D-dimer was 2448 ng/dL, the average lactic dehydrogenase was 538 U/l, and oxygen saturation was 78.54%. These results undoubtedly indicate that the disease caused by COVID-19 can be very severe in high-altitude residents, which is currently controversial since there are studies that propose that the cases in high altitude might not be so severe [14, 15].

The severity of the cases is only comparable to the first deceased cases in the Rebagliati Hospital [19] as well as to the subgroup of those deceased in the Iranian population [17]. Based on these findings, developing a chest CT scan severity score is crucial, as pointed out by Holguín et al. [27], who tested five severity scales after evaluating 35 cases of COVID-19 with a chest CT scan. Due to the small size of the population, they did not reach definitive conclusions except those already known, such as bilateral involvement, simultaneous stages, and pleural effusion, which indicate greater severity. Pulmonary artery diameter was 27.56 mm on average, with a minimum value of 18 and a maximum of 38 mm. The relationship of pulmonary arterial pressure with severity or comorbidities still needs to be evaluated.

Chest CT scan is a valuable tool for COVID-19 identification. According to Liu et al. [28], this ancillary test has 88% to 97% sensitivity for COVID-19 pneumonia diagnosis, superior to the RT-PCR test. Unfortunately, the identification of COVID-19 lesions by CT scan is observer-dependent. According to Bai et al. [29], radiologists have different levels of performance that can go from 67% to 97% sensitivity and from 7% to 100% specificity. This disparity in diagnostic precision can be improved with the use of Artificial Intelligence (AI), as revealed by the studies of Nasir [30] and Mohan et al [31]. In specific settings and using pre-trained transfer learning-based models, AI can reach 99.6% precision [24] for COVID-19 identification. AI has been tested in different areas of the medical profession. The distinction between normal and malignant breast cancer cells using electric circuit networks [32] or the detection of diabetic retinopathy by the employment of Convolutional Neural Networks [33, 34] Biosensors have also proven to be helpful for COVID-19 diagnosis [35], as similar devices have been found useful to identify hematuria [36] or kidney stones [37]. Integrating AI in identifying specific chest CT scan patterns can significantly improve the diagnostic precision of COVID-19 pneumonia.

5. Conclusions

Most cases were classified as CORADS 5 and had great severity according to pulmonary lesions and altered biochemical tests. The prevalence of comorbidities was high, and total lung involvement was 52.03% on average. The most frequently found pattern was ground glass with 93.8%, followed by the alveolar consolidation pattern with 86.2%. In 85.6% of patients, the lesions' distribution was central and peripheral. The lesions found were more severe than in the Chinese studies, comparable with the Spanish and Iranian series. As in most tomographic studies, the most common patterns were bilateral ground glass infiltrates, regularly located in the lower lobes. The presence of paraaortic and subaortic nodes was more frequent than in the rest of the published studies, probably indicating the severity of the condition.

Acknowledgments

The authors wish to thank the authorities of the Regional Surgical Medical "Daniel A. Carrión" Hospital, who gave us the facilities to carry out the study.

Author Contributions

The idea of the manuscript was planned by APS and WCG. The basic literature was brought together and the first draft was prepared by APS and GTS. APS and GTS collected and compiled the information. APS edited the final draft and WCG and GTS approved the final version of the manuscript. All the authors have read and approved the submission of the manuscript.

Competing Interests

The authors have no conflict of interest.

References

1. Phelan AL, Katz R, Gostin LO. The novel coronavirus originating in Wuhan, China: Challenges for global health governance. JAMA. 2020; 323: 709-710.
2. Trilla A. One world, one health: The novel coronavirus COVID-19 epidemic. Med Clin (Engl Ed). 2020; 154: 175-177.
3. Wang D, Hu B, Hu C, Zhu F, Liu X, Zhang J, et al. Clinical characteristics of 138 hospitalized patients with 2019 novel coronavirus-infected pneumonia in Wuhan, China. JAMA. 2020; 323: 1061-1069.
4. Chu DK, Pan Y, Cheng SM, Hui KP, Krishnan P, Liu Y, et al. Molecular diagnosis of a novel coronavirus (2019-nCoV) causing an outbreak of pneumonia. Clin Chem. 2020; 66: 549-555.
5. Salehi S, Abedi A, Balakrishnan S, Gholamrezanezhad A. Coronavirus disease 2019 (COVID-19): A systematic review of imaging findings in 919 patients. AJR Am J Roentgenol. 2020; 215: 1-7.
6. Corman VM, Landt O, Kaiser M, Molenkamp R, Meijer A, Chu DK, et al. Detection of 2019 novel coronavirus (2019-nCoV) by real-time RT-PCR. Eurosurveillance. 2020; 25: 2000045.
7. Kim JY, Choe PG, Oh Y, Oh KJ, Kim J, Park SJ, et al. The first case of 2019 novel coronavirus pneumonia imported into Korea from Wuhan, China: Implication for infection prevention and control measures. J Korean Med Sci. 2020; 35: e61.
8. Pan Y, Guan H, Zhou S, Wang Y, Li Q, Zhu T, et al. Initial CT findings and temporal changes in patients with the novel coronavirus pneumonia (2019-nCoV): A study of 63 patients in Wuhan, China. Eur Radiol. 2020; 30: 3306-3309.
9. Ai T, Yang Z, Hou H, Zhan C, Chen C, Lv W, et al. Correlation of chest CT and RT-PCR testing for coronavirus disease 2019 (COVID-19) in China: A report of 1014 cases. Radiology. 2020; 296: E32-E40.
10. Zu ZY, Jiang MD, Xu PP, Chen W, Ni QQ, Lu GM, et al. Coronavirus disease 2019 (COVID-19): A perspective from China. Radiology. 2020; 296: E15-E25.
11. Chung M, Bernheim A, Mei X, Zhang N, Huang M, Zeng X, et al. CT imaging features of 2019 novel coronavirus (2019-nCoV). Radiology. 2020; 295: 202-207.
12. Song F, Shi N, Shan F, Zhang Z, Shen J, Lu H, et al. Emerging 2019 novel coronavirus (2019-nCoV) pneumonia. Radiology. 2020; 295: 210-217.

13. Xu X, Yu C, Qu J, Zhang L, Jiang S, Huang D, et al. Imaging and clinical features of patients with 2019 novel coronavirus SARS-CoV-2. Eur J Nucl Med Mol Imaging. 2020; 47: 1275-1280.
14. Perez Castilla J. High Altitude and COVID-19: A relationship difficult to assess. Arch Bronconeumol. 2021; 57: 68-70.
15. Zubieta Calleja G, Merino Luna A, Zubieta DeUrioste N, Armijo Subieta NF, Soliz J, Arias Reyes C, et al. Re: "Mortality Attributed to COVID-19 in high-altitude populations" by Woolcott and Bergman. High Alt Med Biol. 2021; 22: 102-104.
16. Aguadero IS, Casajús AE, Ferradas FM, Rouilleault AI, Nuin AP, Villoslada JP, et al. Chest computed tomography findings in different phases of SARS-CoV-2 infection. Radiologia (Engl Ed). 2021; 63: 218-227.
17. Ashtari S, Vahedian Azimi A, Shojaee S, Pourhoseingholi MA, Jafari R, Bashar FR, et al. Computed tomographic features of coronavirus disease-2019 (COVID-19) pneumonia in three groups of Iranian patients: A single center study. Radiologia (Engl Ed). 2021; 63: 314-323.
18. Escobar G, Matta J, Taype W, Ayala R, Amado J. Clinico-epidemiological characteristics of patients deceased by COVID-19 in a National hospital in Lima, Peru. Rev Fac Med Hum. 2020; 20: 180-185.
19. Cui N, Zou X, Xu L. Preliminary CT findings of coronavirus disease 2019 (COVID-19). Clin Imaging. 2020; 65: 124-132.
20. Wu J, Wu X, Zeng W, Guo D, Fang Z, Chen L, et al. Chest CT findings in patients with coronavirus disease 2019 and its relationship with clinical features. Invest Radiol. 2020; 55: 257.
21. Xu YH, Dong JH, An WM, Lv XY, Yin XP, Zhang JZ, et al. Clinical and computed tomographic imaging features of novel coronavirus pneumonia caused by SARS-CoV-2. J Infect. 2020; 80: 394-400.
22. Sharif PM, Nematizadeh M, Saghazadeh M, Saghazadeh A, Rezaei N. Computed tomography scan in COVID-19: A systematic review and meta-analysis. Pol J Radiol. 2022; 87: e1-e23.
23. Zheng Q, Lu Y, Lure F, Jaeger S, Lu P. Clinical and radiological features of novel coronavirus pneumonia. J X-Ray Sci Technol. 2020; 28: 391-404.
24. Ahuja S, Panigrahi BK, Dey N, Rajinikanth V, Gandhi TK. Deep transfer learning-based automated detection of COVID-19 from lung CT scan slices. Appl Intell. 2021; 51: 571-585.
25. Kenny JE, Canepa CM. An illustrated guide to the chest CT in COVID [Internet]. PulmCCM; 2020. Available from: https://pulmccm.org/uncategorized/an-illustrated-guide-to-the-chest-ct-in-COVID-19/PulmCCM.
26. Waller JV, Kaur P, Tucker A, Lin KK, Diaz MJ, Henry TS, et al. Diagnostic tools for coronavirus disease (COVID-19): Comparing CT and RT-PCR viral nucleic acid testing. Am J Roentgenol. 2020; 215: 834-838.
27. Holguín Andrade KI, Murrieta Peralta E, Chischistz Condey AP, Solís Cano DG, Ríos Muñoz R, Calva Arcos M, et al. Inter-observer variability with five computed tomography severity scales for COVID-19 pneumonia assessment. Gac Med Mex. 2021; 157: 391-396.
28. Liu M, Lyu J, Zheng X, Liang Z, Lei B, Chen H, et al. Evolution of the newest diagnostic methods for COVID-19: A Chinese perspective. J Zhejiang Univ Sci B. 2023; 24: 463-484.
29. Bai HX, Hsieh B, Xiong Z, Halsey K, Choi JW, Tran TM, et al. Performance of radiologists in differentiating COVID-19 from non-COVID-19 viral pneumonia at chest CT. Radiology. 2020; 296: e46-e54.

30. Nasir N, Kansal A, Barneih F, Al Shaltone O, Bonny T, Al-Shabi M, et al. Multi-modal image classification of COVID-19 cases using computed tomography and X-rays scans. Intell Syst Appl. 2023; 17: 200160.
31. Mohan N, Kabeer S, Nasir N. Artificial Intelligence (AI) in the diagnosis of COVID-19 Detection: A Review. 2021 28th IEEE International Conference on Electronics, Circuits, and Systems (ICECS); 2021 November 28 - 2021 December 01; Dubai, United Arab Emirates. Piscateville, NJ, US: IEEE.
32. Nasir N, Al Ahmad M. Measuring transmittance of human female breast cells through spectrophotometry and generating its equivalent circuit by prony modelling. In: 2017 4th IEEE International Conference on Engineering Technologies and Applied Sciences (ICETAS). Salmabad, Bahrain: IEEE; 2017. pp. 1-5.
33. Nasir N, Oswald P, Alshaltone O, Barneih F, Al Shabi M, Al Shammaa A. Deep DR: Detection of diabetic retinopathy using a convolutional neural network. In: 2022 Advances in Science and Engineering Technology International Conferences (ASET). Dubai, United Arab Emirates: IEEE; 2022. pp. 1-5.
34. Nasir N, Afreen N, Patel R, Kaur S, Sameer M. A transfer learning approach for diabetic retinopathy and diabetic macular edema severity grading. Rev Intell Artif. 2021; 35: 497-502.
35. Seo G, Lee G, Kim MJ, Baek SH, Choi M, Ku KB, et al. Rapid detection of COVID-19 causative virus (SARS-CoV-2) in human nasopharyngeal swab specimens using field-effect transistor-based biosensor. ACS Nano. 2020; 14: 5135-5142.
36. Nasir N, Raji S, Mustafa F, Rizvi TA, Al Natour Z, Hilal Alnaqbi A, et al. Electrical detection of blood cells in urine. Heliyon. 2020; 6: e03102.
37. Nasir N, Najar A, Al Ahmad M. Optical characterization of calcium oxalate hydrate in urine. In: 2018 IEEE 5th International Conference on Engineering Technologies and Applied Sciences (ICETAS). Bangkok, Thailand: IEEE; 2018. pp. 1-5.